Lawrence Berkeley National Laboratory
Lawrence Berkeley National Laboratory

Title
The structure of the alpha-Al2O3(0001) surface from low-energy electron diffraction: Al termination and evidence for large thermal vibrations

Permalink
https://escholarship.org/uc/item/0cc5z7q2

Authors
Soares, E.A.
Van Hove, M.A.
Walters, C.F.
et al.

Publication Date
2000-05-05

Peer reviewed

The Structure of the α-Al$_2$O$_3$(0001) Surface
from Low-Energy Electron Diffraction:
Al Termination and Evidence for Large Thermal Vibrations

E. A. Soares[*]

Materials Sciences Division, Lawrence Berkeley National Laboratory, Berkeley, CA 94720,

USA,

M. A. Van Hove

Materials Sciences Division and Advanced Light Source,

Lawrence Berkeley National Laboratory, Berkeley, CA 94720, USA, and

Department of Physics, University of California, Davis, CA 95616, USA,

C. F. Walters[**] and K. F. McCarty

Sandia National Laboratories, Livermore, CA 94551, USA

Abstract

We have used dynamical low-energy electron diffraction (LEED) to determine the surface structure of α-Al$_2$O$_3$(0001). Sapphire surfaces were prepared in three different ways, and the diffraction results were analyzed using an exhaustive search of possible models. For all sample processing conditions, the clearly favored structure has a single Al layer termination and a large first interlayer contraction. In addition, we find that the aluminum atoms at the surface have unusually large vibrational amplitudes at room temperature, suggestive of an anharmonic vibrational mode.

*Current address: Instituto de Fisica Gleb Wataghin, UNICAMP, CP 6165, Campinas,
13083-970, Brazil.
**Current address: Novellus Systems Inc., San Jose, CA.

PACS numbers: 61.14.H, 68.35.B, 68.35.J

Introduction

Alumina (i.e., aluminum oxide and its hydrates) is widely used in aluminum production, ceramics, catalysts, and occurs on the surface of oxidized aluminum alloys.[1, 2] Being the simplest and the only thermodynamically stable aluminum oxide,[2] α-Al$_2$O$_3$ is a prototype for understanding metal oxides. Because of its importance, numerous experimental[3-8] and theoretical[9-16] investigations of its surfaces have been performed. Nonetheless, a most basic property of its simplest clean surface, namely the structure of α-Al$_2$O$_3$ (0001), remains controversial.

Compared to mono-atomic materials, determining the surface structure of a compound has several additional complicating factors. First, a compound may terminate along different ideal planes, giving inequivalent surface structures. For α-Al$_2$O$_3$(0001), three different (0001)-plane terminations exist: a single Al layer (Al1), an oxygen layer (O1), and a double Al layer (Al2), where we denote the different surfaces by the terminating layer(s) as labeled in Fig. 1. First-principles calculations predict an Al1 termination with the first interlayer spacing being greatly contracted (~85%) relative to the bulk.[12-16] X-ray-diffraction[6] and ion-scattering[5] experiments concluded that the α-Al$_2$O$_3$(0001) surface is Al1 terminated. However, the models considered in these investigations were limited to the ideal (0001) plane surfaces, i.e., the Al1, O1, and Al2 surfaces. Additionally, these experiments found a first interlayer contraction that is ~35% smaller than that predicted by theory. Based on their calculations of the TiO$_2$(110) surface, Harrison et al. have suggested that the difference in interlayer spacings determined by zero-temperature calculations and room-temperature experiments may be explained by the existence of large, anharmonic vibrations.[17] Since such vibrations cannot be accurately modeled in low-energy electron diffraction (LEED) calculations using an isotropic Debye-Waller approximation, evaluating their existence requires the use of more complex models.[18-20]

In addition to single-species termination, compound surfaces can potentially be phase-separated, i.e., consist of a thermodynamic equilibrium of domains having different stoichiometry or structure.[12, 13, 15, 21]   For example, calculations suggest that under typical experimental conditions, the (0001) surface of the isostructural phase α-Fe$_2$O$_3$ is covered by two distinct domains, one terminated by Fe and one by O.[21] Experimentally, the surface has been reported to consist either of two domains with different structure,[21] or, inconsistently, as exclusively terminated by oxygen.[22]   For α-Al$_2$O$_3$(0001), the three ideal bulk terminations have different stoichiometries at the surface. Therefore, their surface energies depend differently on the oxygen (alumina) chemical potential.[12, 13, 15, 16] Because the single-Al layer (Al1) surface has the same stoichiometry as the bulk, its energy is independent of the aluminum or oxygen chemical potential, unlike the non-stoichiometric surfaces terminated by an oxygen layer or a double Al layer. This raises the possibility that the lowest energy state, for a given chemical potential, is actually a phase-separated mixture of two different surface terminations. Therefore, the existence of a phase-separated surface and the relative amounts of each phase, may depend sensitively on processing conditions. In the α-Fe$_2$O$_3$(0001) system, for example, Shaikhutdinov and Weiss[23] found that changing the ambient oxygen pressure from 1 mbar to 10^{-5} mbar changed the surface structure from being oxygen terminated to being iron terminated. In fact, the previous LEED study on α-Al$_2$O$_3$(0001) concluded that a mixture of Al- and O-terminated domains best modeled the diffraction data.[7]   In contrast, a recent ion-scattering study[8] of the sapphire surface also considered mixed-terminations but concluded that the single-Al-termination model (Al1) best fit the data. Whether phase separation should occur has also been addressed by first-principles calculations. Because the single Al-layer surface (Al1 model) is calculated to have the lowest energy for the full range of chemical potential spanning the decomposition of sapphire at extremely low oxygen pressures up to at least an atmosphere of oxygen, phase separation should be precluded.[12, 13, 15, 16]

A further complication associated with compound structures was noted by Toofan and Watson in a recent LEED study [7] – the α-Al$_2$O$_3$(0001) surface can be terminated by planes that give different diffraction intensities even though the planes are chemically and energetically equivalent. These diffractionally inequivalent planes (e.g., the O1 and O2 planes) are separated by odd multiplies of $c/6$ (where c is the c axis unit-cell length) and only differ in being a mirror image of each other. Then, if a sample has a terrace and step structure with step heights that are odd multiples of $c/6$, the diffraction pattern will have contributions from both terrace types. In fact, terraces separated by $c/6$ have been observed on the α-Al$_2$O$_3$(0001) surface by atomic force microscopy[24, 25] and their existence is consistent with ion-scattering results.[5] Unfortunately, the previous LEED study was performed with an off-normal incident beam and the scattering plane was aligned in such a way as to make the diffractional inequivalence unobservable.[7] In this work, we examine whether these inequivalent terraces significantly affect the simulated LEED spectra.

Finally, the surface of a compound may not be derived from a simple planar cleavage of the bulk. For example, the near-surface layers may have a different stacking sequence than the bulk, yet maintain the surface symmetry observed by LEED. Such stacking faults were considered in a recent LEED analysis of another corundum-type structure, α-Cr$_2$O$_3$(0001).[26] The consideration of such models is particularly relevant for α-Al$_2$O$_3$(0001) because the related spinel phase γ-Al$_2$O$_3$ may have a lower surface energy.[10] A structure like γ-Al$_2$O$_3$ would occur on the surface if the O stacking sequence of α-Al$_2$O$_3$(0001) changed from the usual hcp-type (*ABABA...*) to one where the final O layer was shifted to the *C* site (*CBABA...*).

Here we present a detailed account of our structural study of the α-Al$_2$O$_3$(0001) surface, a brief version of which has already been published.[27] Given the discussion above, we emphasize both the sensitivity of the surface to sample preparation effects and the completeness of the structural analysis. These two issues are related due to the fact that, in the case of *compounds*, sample preparation can affect both surface stoichiometry and structure,[28] and the structure will be

correctly determined only if the appropriate class of structural model is considered. Understanding these issues is of central importance in advancing surface science and its applications because so many materials of technological importance are compounds.

Experimental details

The sapphire crystal was first annealed in air in a high-purity furnace at about 1425°C for 12 hours. The furnace consisted of a sapphire tube around which a heating element of Pt/30%Rh wire was wrapped. The tube ends were capped with sapphire plugs. The annealing procedure produced a surface with large terraces (~1000 Å in width), as evidenced by atomic force microscopy. The crystal was then sequentially cleaned in acetone, methanol, 1 M HCl, and deionized water. After the sample was introduced into the vacuum chamber, residual carbon contamination was removed at 650°C using an atomic deuterium beam created by a commercial, neutralized, rf plasma discharge.[29] To investigate the sensitivity of surface structure to processing conditions, we finished the processing in three very different ways: 1) turn off the atomic deuterium beam and cool from 650°C in vacuum ("Vac" data), 2) cool to 200°C before turning off the atomic deuterium beam ("D" data), and 3) turn off the atomic deuterium beam, heat for 5 min. in 5×10^{-5} Torr O_2, and then cool in vacuum ("Ox" data). All three procedures produced bright, sharp, (1x1) LEED patterns with clear 3-fold symmetry.

The LEED data were acquired with the sample at room temperature using a high-sensitivity CCD camera and an automated data acquisition system. Nine inequivalent beams were recorded at normal incidence in the energy range of 80 to 370 eV (total range 2080 eV). After subtracting the background, defined by the average intensity in the pixels surrounding the region of integration for each beam, equivalent beams were averaged. The spectra were scaled to the incident electron current, which was set low enough to prevent non-linear charging effects (~0.3 μA). Because of the high quality of the data, no mathematical smoothing was required prior to the analysis. Representative experimental LEED I(V) curves (diffracted intensity as a function

of electron energy) for the 3 different sample preparation procedures are shown in Fig. 2. Although the 3 sets are closely similar, we perform independent structural analyses using each data set individually.

Model descriptions

While the corundum structure of bulk α-Al_2O_3 has rhombohedral symmetry, the atomic positions are usually given in terms of an hexagonal unit cell (Fig. 1).[4] This unit cell can be viewed as a sequence of twelve Al layers, which are translationally equivalent to each other, and six O layers, with the O atoms in positions close to those of an hcp lattice. For the six O layers, alternate layers are translationally equivalent, and sequential layers are equivalent *only* after a translation and mirroring through a plane perpendicular to the surface. Any of these 18 layers may serve as a surface termination, and each of these surfaces has p3 symmetry, i.e., 3-fold rotational axes through the Al atoms and no mirror planes. However, while a surface that terminates in layers {Al1-O1-...} is energetically equivalent to one that terminates in layers {Al3-O2-...}, through a symmetry transformation, the mirror-symmetry relationship of the adjacent O layers results in these terminations being inequivalent from the point of view of diffraction. That is, separate regions of Al1 termination and Al3 termination could coexist as energetically-equivalent but diffractionally-inequivalent terraces, and these must be averaged over to correctly model a terraced surface.

The simplest models used to analyze our LEED I(V) data were the ideal planar cleavages: models Al1, O1, and Al2 (see Table 1). A closely related, but non-ideal, model consists of an O atom on top of each surface Al atom of the Al1 model. Since the scattering power of hydrogen is small enough to be neglected, this model represents a type of water- or hydroxyl-covered surface. The next level of complexity involves surfaces that terminate in a single species (i.e., Al atoms or O atoms) but contain diffractionally-inequivalent domains. That is, in these models, the surface consists of the two distinct terrace types (separated by a $c/6$ length along the c-axis). In all of

7

these models (Al1+Al3, O1+O2, Al$_m$, and O$_m$), the fractional coverage of each terrace type was treated as a fitting parameter. For the Al$_m$ and O$_m$ models, the atoms in the "mirrored" (i.e., $c/6$ separated) domains were constrained to have the same relative positions (i.e., mirrored domains were kept identical). In the Al1+Al3 and O1+O2 models, the atoms in the diffractionally-inequivalent terraces (i.e., Al1 and Al3; O1 and O2) were not constrained to have the same relative positions.

We also considered mixed-species models, i.e., surfaces having regions terminated by oxygen atoms and regions terminated by aluminum atoms. In four of these models (Al1+O1, Al1+O2, O1+Al3, and O1+Al2), the fractional coverage of the aluminum-terminated and oxygen-terminated domains and the atomic positions on each domain were independently varied. Finally, we considered a mixed-species model that also had diffractionally inequivalent steps, (Al$_m$)+(O$_m$). The surface fraction occupied by the two inequivalent Al-terminated domains (Al1 and Al3) and the fraction occupied by the two inequivalent O-terminated domains (O1 and O2) were varied. However, to limit the number of adjustable parameters in this "mixed-mirrored surface," the atomic positions within both O-terminated domains and within both Al-terminated domains were constrained to be the same and the two O-terminated domains had equal abundance, as did the two Al-terminated domains (i.e., Al1:Al3 = O1:O2 = 50:50).

All of the previously discussed models are derived by cleaving the bulk structure along appropriate plane(s). However, it is possible that the surface differs from the usual bulk stacking sequence yet has the observed surface symmetry. Therefore, we considered five models that have stacking faults in the topmost one or two layers. Figure 1 shows the stacking of the Al and O layers with the usual notation associated with close-packed structures. The oxygen sublattice follows hcp-type packing (*ABAB*...) while the Al sublattice follows the fcc-type packing (*cbacba*...). As illustrated in Fig. 3, the two simplest stacking-fault structures involve rigidly shifting the top Al layer in the Al1 model from the *c* site (which is not occupied by the two Al

layers located between layers O1 and O2) to either the *a* site or the *b* site (both of which are occupied by Al atoms located between layers O1 and O2). The second type of stacking fault involves shifting the O1 layer from the *B* site to the *C* site, along with removing the distortion of the layer such that it has perfect hexagonal symmetry. The upper three oxygen layers then have fcc-type stacking, as in the cubic phase γ-Al_2O_3. In addition, the aluminum atoms in the Al2 and Al3 layers occupy tetrahedral sites, unlike the exclusive octahedral occupancy of α-Al_2O_3. Three different structures follow from the O stacking fault (Fig. 3), namely, terminating in the O1 layer (i.e., the Al1 layer is absent, model 9), placing the Al1 layer in the three-fold hollow sites directly below which there are no atoms (model 10), and placing the Al1 layer in the three-fold hollow sites directly above the O atoms of the O2 layer (model 11).

Finally, we have considered the possibility that the surface Al atoms in the theoretically favored Al1 model have anisotropic vibrations that cannot be correctly described using the isotropic Debye-Waller factor to which the standard LEED calculations are limited. If this is the case, the Al1 model will result in a poor fit to the data even if the surface is in fact terminated by a single Al layer. To investigate this possibility, we modeled the surface with the well-established "split-position" technique,[18-20] by constructing an equal mixture of two identical Al-terminated domains in which the topmost interlayer spacing is allowed to independently relax. (This model allows the split atoms to be half the time in one position and half the time in the other position, thereby simply representing a large vibrational amplitude perpendicular to the surface.) If the vibrational amplitude perpendicular to the surface is indeed too large to be correctly modeled by an isotropic Debye-Waller factor, the spacing between the split surface atoms in the two domains will increase, while the position of all other atoms in the model will be very similar.
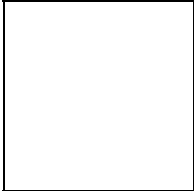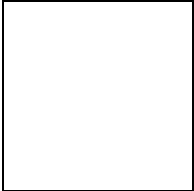
LEED calculational technique

The LEED analysis applied the familiar method of symmetrized automated tensor LEED,[30] which has been used, for example, to study the complex oxide $Fe_3O_4(111)$.[31, 32] Although α-Al_2O_3 is an ionic compound, neutral scattering phase shifts were used. It is well known that the structural fit depends very little on those non-structural parameters, provided their values are reasonable. This point was explicitly checked by Barbieri et al.[31] in the surface structural analysis of $Fe_3O_4(111)$. To take into account the difference in the ionic radii, we assumed that the oxygen muffin-tin radius (r^O_{muf}) was twice the Al muffin-tin radius ($r^O_{muf} = 2r^{Al}_{muf}$). The muffin-tin potential and the phase shifts were calculated using the Barbieri/Van Hove Phase Shift Package.[33] In particular, a self-consistent Dirac-Fock approach was used to compute the self-consistent atomic orbitals for each element. The muffin-tin potential was then computed following Mattheis' prescription and the relativistic phase shifts were evaluated by numerical integration of the Dirac equation.

In all of the models we tested, the atoms were allowed to fully relax down to a depth of 7 layers under the provision that they maintain the observed p3 symmetry. Under this constraint, atoms that lie along the axis passing through the bulk Al atoms can only relax perpendicular to the surface, while other atoms could also relax laterally. In all cases where mixed domains were considered, the calculated spectra were derived from incoherently summing over the different terraces.

The goodness of the fits to the various structural models is described in terms of the Pendry R-factor (R_p).[34] One additional criterion, known in x-ray crystallography as the Hamilton-ratio test,[35, 36] is herein introduced to LEED to deal with variable numbers of fit-parameters, as occurs when comparing a model that consists of a single structure with a model that consists of more than one structure. The Hamilton ratio helps to distinguish real improvements in a fit due to choosing a better model, from artificial improvements due only to fitting more structural

parameters. As long as the structural coordinates are otherwise reasonable, a large Hamilton ratio is indicative of real improvements. Adapted to the LEED case, the Hamilton ratio is defined as:

$$H_r = \frac{(R_s^2 - R_{mix}^2)(n - p)}{R_{mix}^2(p - q)}, \text{ (is this right?)}$$

where [   ] and [   ] are the R-factors for the model with the smaller (p_{small}) (is this right?) and larger (p_{large}) (is this right?) number of fitting parameters, and n is the number of diffraction peaks. In a LEED-I(V) spectrum, the width of the dominant peak is about $2|V_{oi}|$, where V_{oi} is the inner potential. In addition, the I(V) curves usually contain as many peaks as can possibly be fit into the available energy range. Therefore, we assume that the number of diffraction peaks n is reasonably estimated by the total energy range divided by the peak width. In our experience this formulation is applicable to all the various R-factors commonly used in LEED, and the ratio should exceed 3 to indicate real improvements.

Results

For each of the three different sample preparations, we have performed the most exhaustive structural examination of α-Al$_2$O$_3$(0001) to date by examining 21 different surface models within six distinct model classes (Table 1). The results of the optimized fitting of the various structural models are summarized in Fig. 4 in terms of the Pendry R-factor (R_p) and the Hamilton ratio (H_r). We are looking for structures with a low R_p, preferably lower by 20% than other structures, and with a relatively large Hamilton ratio, preferably larger than 3. Additionally, we need to exclude physically unrealistic structures, namely those that have unacceptable bond lengths. These structures are indicated by a pound sign in Fig. 4.[37] None of the ideal terminations (models 1-5) or the "hydroxyl" surface (model 6) adequately describes the data. The single-species models that included diffractionally inequivalent domains (models 12-15) also gave unacceptable R_p values or unphysical bond lengths. This fact establishes that the aluminum-terminated surface model (Al1) is not inadequate simply because the diffractionally inequivalent

terraces have not been considered. Clearly, additional effects beyond diffractionally inequivalent domains must be included to adequately model the LEED data. In models Al1+Al3 and O1+O2 (models 12 and 13), there are additional degrees of freedom available because the relative atomic positions on the two domains are not constrained to be the same. The fitting has artificially used these degrees of freedom to produce low R_p values by making unphysical bond lengths. That these fits are artificial is also reflected in the low Hamilton ratios for these models.

The split-position (model 21) and Al1+O1 mixed-termination (model 16) models are clearly favored over the other models, irrespective of the surface preparation, based upon their low Pendry R-factors and high Hamilton ratios. For all three preparation methods, the Al1-split model has the lowest R_p's and the highest H_r's. However, since the Al1+O1 model has R_p values that are only ~10% larger and has acceptable H_r values, this model cannot be immediately discarded. However, additional considerations that are discussed below allow us to clearly favor the Al1-split model.

The best-fit Al1+O1 model has several questionable properties. First, fitting the two "cleanest" preparation methods (Ox and Vac) with the model gave surfaces that are essentially bulk-like, while the preparation method that involved exposure to deuterium (D data) at low temperatures produced a significant contraction of the first interlayer spacing (see Fig. 5 and Table 2). This is counter to the usual expectation that clean surfaces are contracted, and that the adsorption of hydrogen results in a return of the first-interlayer spacing to one that resembles the bulk value.[38, 39] Second, the Al1+O1 models were extremely insensitive to the relative amounts of Al and O domains. In fact, the uncertainty in the mix ratio is on the order of ±40% for all three preparation methods, as can be seen from Fig. 6 for the case of the D data. This insensitivity is physically very unsatisfying. Finally, the Al1+O1 model is entirely inconsistent with theoretical predictions for the clean surface, which show that the Al1 model has lowest energy over sapphire's full range of stability,[12, 13, 15] precluding a phase-separated surface such as the Al+O

models. Figure 6 also shows that the same insensitivity of R_p to composition is obtained for other mixed-domain models considered in this work. Again, similar R_p behavior was also observed for the other two sample preparation procedures.

In contrast, the simpler Al1-split model gives consistent and physically reasonable results. As seen in Fig. 5, the only significant difference between the two domains is the separation of the top Al layer. This supports the validity of the model since the additional degrees of freedom in the layers below the surface could have been used to give a good fit. That is, if the model was unsuitable, the domains would differ significantly beyond the first layer, using these additional degrees of freedom to best fit the data. This observation is also consistent with the split-position model having a Hamilton ratio larger than all the other models. In the split-position method, the difference in the position of the Al atoms in the two domains is related to the vibrational amplitude of the outermost Al atoms. The large difference we observe, ~0.24 Å, is indicative of an anharmonic enhancement of the perpendicular vibrational mode of the outermost Al surface atoms.[40] In addition, the Al1-split model has an average first-interlayer spacing that is in reasonable agreement with the previous x-ray[6] and ion-scattering[5] measurements. Importantly, the fact that our three sample-preparation methods result in essentially the same surface structure shows that the α-Al_2O_3(0001) surface is very stable and insensitive to processing conditions. The experimental and theoretical LEED I(V) curves using the split-position model for the Ox data set are presented in Fig. 7. The same level of agreement between theory and experiment was obtained for the two other experimental data sets.[41]

Although the uncertainties in the displacements parallel to the surface are larger compared to the perpendicular ones, our results suggest a small rotation of the oxygen atoms in the first oxygen layer (O1). As shown in Table 2, this work's values are in reasonable agreement with those obtained by and x-ray diffraction experiments and first-principle calculations. A diagram of

the best structure for the split-position model is presented in Fig. 8. The coordinates are the average of the atomic coordinates of the two Al domains presented in Table 3.

Discussion

While we find a large interlayer contraction at the surface, the contraction is significantly smaller than that predicted from state-of-the-art calculations.[12, 13, 15] Since recent first-principles calculations[15, 16] have shown that hydrogen absorption on the aluminum-terminated surface reduces the contraction close to the value of this and other experimental studies,[5, 6] we next discuss hydrogen on the α-Al$_2$O$_3$(0001) surface.

The α-Al$_2$O$_3$(0001) surface is actually quite difficult to hydroxylate. While water undergoes dissociative chemisorption on the α-Al$_2$O$_3$(0001) surface, extensive hydroxylation occurs only for vapor pressures above about 1 Torr.[42] For vapor pressures below 1 Torr, water adsorption produces only limited amounts of surface hydroxyl, presumably mainly at defect sites.[42] The fully hydrated surface has been shown experimentally to be oxygen terminated.[43, 44] First-principles calculations show that this surface is thermodynamically stable only for substantial pressures of H$_2$ or water.[13, 15, 16] Furthermore, surface hydroxyl species are readily removed at very modest temperatures. Laser-induced thermal desorption and temperature-programmed desorption have shown that the hydroxyl coverage is negligible above 500K.[45] Consistently, Coustet and Jupille found that their cleaning procedure of heating to 1000K fully desorbed surface hydroxyl, as directly evidenced by vibrational (electron-energy-loss) spectroscopy.[46] Clearly, then, our "Vac" (heating in vacuum at 650°C) and "Ox" (heating in O$_2$ at 650°C) procedures should produce hydroxyl-free surfaces.

These experimental results are in conflict with a recent ion-scattering study, which concluded that substantial amounts of hydrogen existed on the α-Al$_2$O$_3$(0001) surface even after heating to 1100°C.[5] The only way to resolve this contradiction with the desorption and

14

vibrational-spectroscopy studies is if hydrogen exists in a non-hydroxyl form on the surface. While we cannot totally discount this possibility, it seems unlikely for several reasons. To begin with, there are only two thermodynamically stable surfaces -- the clean (hydrogen-free) aluminum-terminated surface (at low hydrogen chemical potentials) and the fully hydrated surface (at high hydrogen chemical potentials).[15] While hydrogen is calculated to bond directly to aluminum atoms of the Al-terminated surface (making a non-hydroxyl species) at 0 K, the bonding is weak.[15] Indeed, simulations at room temperature using first-principles molecular dynamics revealed only OH species, not Al-H species.[47, 48] Given these observations, it is surprising that hydrogen can remain on the surface at 1100°C,[5] the approximate temperature at which substantial oxygen loss from the surface begins, leading to surface reconstructions.[49, 50] Why hydrogen would be more strongly bound then oxygen is unclear. Finally, the source of the surface hydrogen is also unclear -- the bulk hydrogen concentration is extremely low in high-quality sapphire.[51] Clearly, more experimental work needs to be done on the hydrogen concentration of the α-Al$_2$O$_3$(0001) surface at elevated temperatures.

While the majority of experimental and theoretical results suggest that the (0001) surface of α-Al$_2$O$_3$ should be relatively free of hydrogen after heating in vacuum, it is not possible at this time to totally discount the presence of any hydrogen. However, it can be argued that hydrogen/hydroxyl is not responsible for the discrepancy between theory and experiment regarding the degree of surface contraction. Our current results find essentially the same surface structure (degree of contraction) despite three quite different processing conditions. Furthermore, our inward relaxation of about 51% agrees well with the values determined by the ion-scattering[5] (63%) and x-ray diffraction[6] (51%) studies. Presumably, our different processing conditions and the other procedures used elsewhere would produce varying amounts of hydrogen/hydroxyl contamination, which would be manifested in differing surface contractions. Our analysis, however, does suggest a possible physical origin for the discrepancy between theory and experiment.

In general, the vibrations of surface atoms are 30-40% larger than those in the bulk. However, using the Debye temperature for the Al atoms derived from the LEED-I(V) calculations (350 K), we calculate a bulk vibrational amplitude of 0.12 Å at room temperature. Our results suggest that the vibrational amplitude perpendicular to the surface is very large, about 0.24Å. Thus, the vibrational amplitude at room temperature is approximately 100% greater than the bulk value. While surprising, this result is not without precedent -- large vibrations have been observed on other surfaces, e.g., Be(0001),[52] Ag(111),[53] Cu(111),[54] and $H_2O(0001)$,[55, 56] and have also been predicted, but not yet detected, for oxides.[17, 57] Furthermore, as suggested by Harrison et al., the discrepancy between theory and experiment over the amount of first-layer contraction may result from the failure of the zero-temperature calculations to account for large surface vibrations.[17] (In the TiO_2 (110) surface structure determined by x-ray diffraction,[58] the topmost oxygen row is actually contracted significantly *more* than predicted by first-principles calculations.[17]) Such large vibrations may have important implications for understanding the detailed surface properties of metal oxides. In the sapphire case, the presence of enhanced vibrations at the surface is easily visualized in terms of the reduced coordination -- the Al-O bonds of the surface Al atoms are almost parallel to the surface, and thus the vibrations are primarily governed by bond-angle changes, which are generally softer than bond-length changes.

Summary

We have studied the α-Al_2O_3(0001) surface structure by examining an unprecedented number of model structures and emphasizing the sensitivity to the sample preparation method. We conclude that the surface termination of α-Al_2O_3(0001) is a single Al layer, that the first interlayer spacing is significantly contracted with respect to the bulk spacing, and that the surface structure is insensitive to our different processing methods, thus resolving contradictory experimental results in the literature. In addition, we suggest that the topmost Al layer has unusually large vibrational amplitudes at room temperature. Such vibrations may account for the

substantial difference between the interlayer contractions determined by zero-temperature calculations and finite-temperature experiments.

References

[1] H. J. Freund, H. Kuhlenbeck, and V. Staemmler, Rep. Prog. Phys. **59**, 283 (1996).

[2] L. D. Hart (Ed.), *Alumina chemical science and technology handbook* (American Ceramic Society Inc., Westerville, OH, 1990).

[3] C. C. Chang, J. Appl. Phys. **39**, 5570 (1968).

[4] T. M. French and G. A. Somorjai, J. Phys. Chem. **74**, 2489 (1970).

[5] J. Ahn and J. W. Rabalais, Surf. Sci. **388**, 121 (1997).

[6] P. Guénard, G. Renaud, A. Barbier, and M. Gautier-Soyer, Surf. Rev. Lett. **5**, 321 (1998).

[7] J. Toofan and P. R. Watson, Surf. Sci. **401**, 162 (1998).

[8] T. Suzuki, S. Hishita, K. Oyoshi, and R. Souda, Surf. Sci. **437**, 289 (1999).

[9] I. Manassidis and M. J. Gillan, J. Am. Ceram. Soc. **77**, 335 (1994).

[10] J. M. McHale, A. Auroux, A. J. Perrotta, and A. Navrotsky, Science **277**, 788 (1997).

[11] V. E. Puchin, J. D. Gale, A. L. Shluger, E. A. Kotomin, J. Gunster, M. Brause, and V. Kempter, Surf. Sci. **370**, 190 (1997).

[12] I. Batyrev, A. Alavi, and M. W. Finnis, Faraday Discuss., 33 (1999).

[13] R. Di Felice and J. E. Northrup, Phys. Rev. B **60**, 16287 (1999).

[14] C. Verdozzi, D. R. Jennison, P. A. Schultz, and M. P. Sears, Phys. Rev. Lett. **82**, 799 (1999).

[15] P. D. Tepesch and A. A. Quong, Phys. Status Solidi B **217**, 377 (2000).

[16] X. G. Wang, A. Chaka, and M. Scheffler, Phys. Rev. Lett. **84**, 3650 (2000).

[17] N. M. Harrison, X.-G. Wang, J. Muscat, and M. Scheffler, Faraday Discuss., 305 (1999).

[18] T. Hertel, H. Over, H. Bludau, M. Gierer, and G. Ertl, Phys. Rev. B **50**, 8126 (1994).

[19] H. Over, W. Moritz, and G. Ertl, Phys. Rev. Lett. **70**, 315 (1993).

[20] C. Stampfl, M. Scheffler, H. Over, J. Burchhardt, M. Nielsen, D. L. Adams, and W. Moritz, Phys. Rev. B **49**, 4959 (1994).

[21] X. G. Wang, W. Weiss, S. K. Shaikhutdinov, M. Ritter, M. Petersen, F. Wagner, R. Schlögl, and M. Scheffler, Phys. Rev. Lett. **81**, 1038 (1998).

[22] S. Thevuthasan, Y. J. Kim, S. I. Yi, S. A. Chambers, J. Morais, R. Denecke, C. S. Fadley, P. Liu, T. Kendelewicz, and G. E. Brown, Surf. Sci. **425**, 276 (1999).

[23] S. K. Shaikhutdinov and W. Weiss, Surf. Sci. **432**, L627 (1999).

[24] J. R. Heffelfinger, M. W. Bench, and C. B. Carter, Surf. Sci. **370**, L168 (1997).

[25] L. Pham Van, O. Kurnosikov, and J. Cousty, Surf. Sci. **411**, 263 (1998).

[26] F. Rohr, M. Baumer, H. J. Freund, J. A. Mejias, V. Staemmler, S. Muller, L. Hammer, and K. Heinz, Surf. Sci. **372**, L291 (1997).

[27] C. F. Walters, K. F. McCarty, E. A. Soares, and M. A. Van Hove, Surf. Sci. **464**, L732 (2000).

[28] V. E. Henrich and P. A. Cox, *The Surface Science of Metal Oxides* (Cambridge University Press, Cambridge, 1996).

[29] C. Heinlein, J. Grepstad, H. Riechert, and R. Averbeck, Mater. Sci. Eng. B **43**, 253 (1997).

[30] Barbieri/Van Hove SATLEED package: http://electron.lbl.gov/.

[31] A. Barbieri, W. Weiss, M. A. Van Hove, and G. A. Somorjai, Surf. Sci. **302**, 259 (1994).

[32] W. Weiss, A. Barbieri, M. A. Van Hove, and G. A. Somorjai, Phys. Rev. Lett. **71**, 1848 (1993).

[33] Barbieri/Van Hove Phase Shift Package: http://electron.lbl.gov/leedpack/leeadpack.hmtl.

[34] J. B. Pendry, J. Phys. C **13**, 937 (1980).

[35] W. C. Hamilton, Acta Crystall. **18**, 502 (1965).

[36] E. Prince, *Mathematical Techniques in Crystallography and Materials Science* (Springer-Verlag, New York, 1982).

[37] Although the Al+O2 and O2+Al3 models (numbered 17 and 18, respectively) have acceptable R_p's and H_r's, their final configurations are close to that of the optimized Al1+O1 model. Therefore, we discuss only the Al1+O1 model.

[38] *The Structure of Surfaces III*, edited by S. Y. Tong, M. A. Van Hove, K. Takayanagi and X. D. Xie (Springer-Verlag, 1991).

[39]   P. R. Watson, M. A. Van Hove, and K. Herman, *NIST Surface Structure Database, Version 3.0, NIST Standard Reference Data Program*, 1999).

[40]   We emphasize that we are not implying that there are two distinct types of surface Al atoms. Instead, we use two Al domains in the split-position model to overcome the inability of the LEED simulations to model highly anisotropic vibrations. Physically, the atomic positions derived are simply the average positions of the two domains.

[41]   While including the diffractionally inequivalent terraces in the split-position model may have lowered the Pendry R-factor, we believe that the structural results would not be significantly altered.

[42]   P. Liu, T. Kendelewicz, G. E. Brown, E. J. Nelson, and S. A. Chambers, Surf. Sci. **417**, 53 (1998).

[43]   P. J. Eng, T. P. Trainor, G. E. Brown, G. A. Waychunas, M. Newville, S. R. Sutton, and M. L. Rivers, Science **288**, 1029 (2000).

[44]   Since we also considered essentially this model (O1) and found it to be unacceptable, clearly our surface was not fully hydrated.

[45]   C. E. Nelson, J. W. Elam, M. A. Cameron, M. A. Tolbert, and S. M. George, Surf. Sci. **416**, 341 (1998).

[46]   V. Coustet and J. Jupille, Nuovo Cimento **19 D**, 1657 (1997).

[47]   K. C. Hass, W. F. Schneider, A. Curioni, and W. Andreoni, Science **282**, 265 (1998).

[48]   K. C. Hass, W. F. Schneider, A. Curioni, and W. Andreoni, J. Phys. Chem. B **104**, 5527 (2000).

[49]   M. Gautier, G. Renaud, L. P. Van, B. Villette, M. Pollak, N. Thromat, F. Jollet, and J. P. Duraud, J. Am. Ceram. Soc. **77**, 323 (1994).

[50]   G. Renaud, B. Villette, I. Vilfan, and A. Bourret, Phys. Rev. Lett. **73**, 1825 (1994).

[51]   A. K. Kronenberg, J. Castaing, T. E. Mitchell, and S. H. Kirby, Acta Mater. **48**, 1481 (2000).

[52] K. Pohl, J.-H. Cho, K. Terakura, M. Scheffler, and E. W. Plummer, Phys. Rev. Lett. **80**, 2853 (1998).

[53] P. Statiris, H. C. Lu, and T. Gustafsson, Phys. Rev. Lett. **72**, 3574 (1994).

[54] K. H. Chae, H. C. Lu, and T. Gustafsson, Phys. Rev. B **54**, 14082 (1996).

[55] N. Materer, U. Starke, A. Barbieri, M. A. Van Hove, G. A. Somorjai, G. J. Kroes, and C. Minot, J. Phys. Chem. **99**, 6267 (1995).

[56] N. Materer, U. Starke, A. Barbieri, M. A. Van Hove, G. A. Somorjai, G. J. Kroes, and C. Minot, Surf. Sci. **381**, 190 (1997).

[57] J. Braun, A. Glebov, A. P. Graham, A. Menzel, and J. P. Toennies, Phys. Rev. Lett. **80**, 2638 (1998).

[58] G. Charlton, P. B. Howes, C. L. Nicklin, P. Steadman, J. S. G. Taylor, C. A. Muryn, S. P. Harte, J. Mercer, R. McGrath, D. Norman, T. S. Turner, and G. Thornton, Phys. Rev. Lett. **78**, 495 (1997).

Tables

Table 1. List of the 21 different models within six different model classes considered in this study of the α-Al$_2$O$_3$(0001) surface. Each model is numbered and given a descriptive notation. When the model considers more than one domain, the experimental data were fit by varying the fractions of the domains, as suggested in the notation.

Model Class	**Model**
Single-species bulk termination	1) Al1
	2) Al2
	3) Al3
	4) O1
	5) O2
	6) Al1-O $\equiv$ "hydroxyl"

Single-species termination with stacking fault	7) Terminated by Al1 on b site
	8) Terminated by Al1 on a site
	9) Terminated by O1 on C site
	10) O1 on C site, terminated by Al1 above "open" site
	11) O1 on C site, terminated by Al1 above O2 sites

Single-species termination with diffractionally inequivalent domains	12) Al1+Al3 $\equiv$ x·Al1+(1-x)·Al3
	13) O1+O2 $\equiv$ x·O1+(1-x)·O2
	14) Al$_m$ $\equiv$ x·Al1+(1-x)·Al3, same relative positions each domain
	15) O$_m$ $\equiv$ x·O1+(1-x)·O2, same relative position each domain

Mixed-species termination	16) Al1+O1 $\equiv$ x·Al1+(1-x)·O1
	17) Al1+O2 $\equiv$ x·Al1+(1-x)·O2
	18) O1+Al3 $\equiv$ x·O1+(1-x)·Al3
	19) O1+Al2 $\equiv$ x·O1+(1-x)·Al2

Mixed-species termination with diffractionally inequivalent domains	20) (Al$_m$)+(O$_m$) $\equiv$ x·(Al1+Al3)+(1-x)·(O1+O2), same relative positions each domain

Split-position	21) Al1-split $\equiv$ Al1+Al1

Table 2. Pendry R-factors R_p, Hamilton ratios H_r and the change in the first two interlayer spacings (with representative uncertainties) for the best fits to models Al1+O1 and Al1-split, for the three sample preparations. For Al1-split, and the Al domains of the Al1+O1 models, Δd_{12} is the Al1-O1 spacing (averaged for Al1-split) and Δd_{23} is the O1-Al2 spacing (averaged for Al1-split). For the O domain of the Al1+O1 model, Δd_{12} is the O1-Al2 spacing, and Δd_{23} is the Al2-Al3 spacing. Also shown are the changes in the first two interlayer distances provided by x-ray diffraction and theory. The rotation of the oxygen atoms in the first oxygen layer (O1) obtained from LEED (this work), from x-ray diffraction experiments and from first-principle calculations is also shown.

	R_p	H_r	Δd_{12} (%)	Δd_{23} (%)	O1 rot. (^{O})	O1 exp. (%)
Al$_1$+O$_1$ (Ox)	0.33	3.58				
Al domain			+5.0±8.0	+0.2±7.0		
O domain			+2.4	-11.8		
Al$_1$+O$_1$ (Vac)	0.33	3.03				
Al domain			0.0	+5.0		
O domain			-1.7	-14.8		
Al$_1$+O$_1$ (D)	0.32	3.96				
Al Domain			-38.4	+7.5		
(O domain)			0.0	-20.2		
Al$_1$-split (Ox)	0.30	4.13	-52.8±5.0	+1.5±5.0	2.7	6
Al$_1$-split (Vac)	0.29	3.88	-50.0	+6.3	3.2	4
Al$_1$-split (D)	0.29	4.55	-50.6	+5.8	2.8	6
X-Ray[6]			-50.8	+16.0	6.7	4.2

Theory[14]			-87.4	+3.1	3.05	3.20

Table 3: Interlayer spacings for the "split-position" model for all three sample preparation procedures.

	Ox data		D data		Vac data	
	1st domain	2nd domain	1st domain	2nd domain	1st domain	2nd domain
$d_{(Al1-O1)}$(Å)	0.25	0.54	0.2738	0.5594	0.2902	0.5520
$d_{(O1-Al2)}$(Å)	0.87	0.84	0.9042	0.8788	0.9318	0.8597
$d_{(Al2-Al3)}$(Å)	0.26	0.28	0.2722	0.2473	0.3073	0.3263
$d_{(Al3-O2)}$(Å)	0.87	0.91	0.9205	0.9009	0.8799	0.8971
$d_{(O2-Al4)}$(Å)	0.79	0.77	0.9205	0.7857	0.8810	0.8065
$d_{(Al4-Al5)}$(Å)	0.55	0.4981	0.4916	0.5583	0.4874	0.5176
$d_{(Al5-Ob)}$(Å)	0.81	0.8355	0.8113	0.8237	0.7947	0.8377
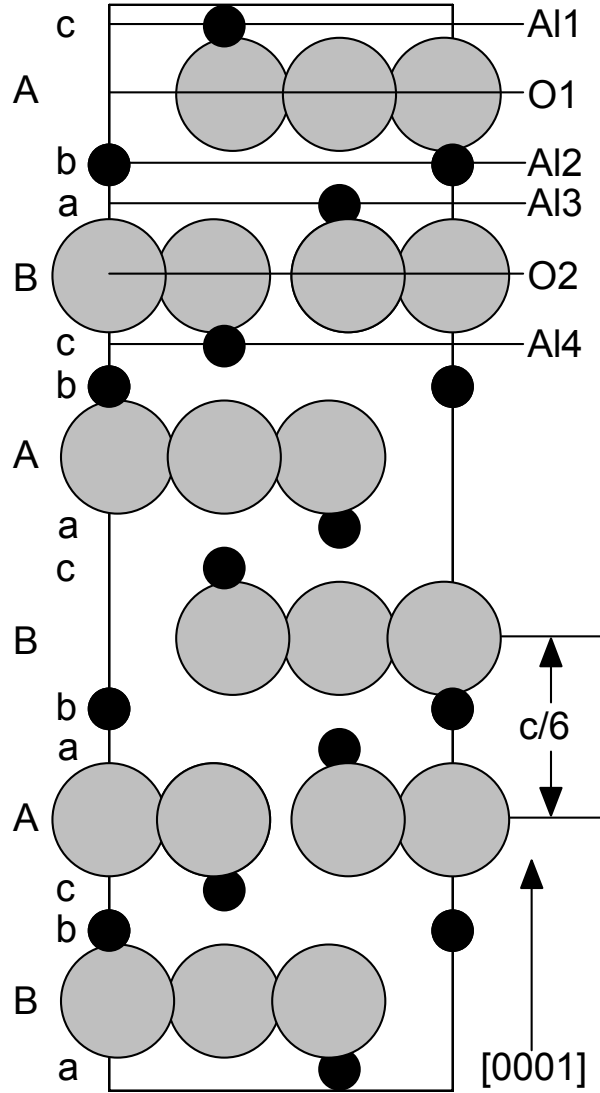
FIG. 1. Illustration of the 12 Al layers and the 6 O layers of the α-Al_2O_3 hexagonal unit cell. The O layers follow approximately hcp-type stacking (*ABAB*...), and the Al layers follow fcc-type stacking (*abcabc*...). Oxygen layers separated by *c*/6 along the *c*-axis are equivalent only after a mirror operation, a symmetry operation that does not pertain to the unit cell as a whole. Thus O layers separated by *c*/6 are diffractionally inequivalent. The planes labeled Al1, O2, and Al2 can all serve as ideal (bulk-like) terminations for the (0001) surface.
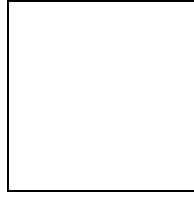
FIG. 2. Representative experimental LEED I(V) curves for the three different sample preparation procedures of the α-Al$_2$O$_3$(0001) surface. The (i,j) notation gives the index of the diffraction spots.
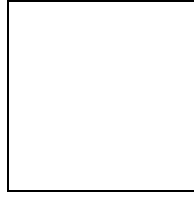
FIG. 3. Schematic illustrations showing the stacking sequence perpendicular to the surface of five stacking-fault models consistent with the observed p3 symmetry. The dashed lines connect atoms that lie on top of each other. Model 1 (the "Al1" model, upper left) maintains the bulk stacking (see Fig. 1). In models 7 and 8, the top most Al layer has been shifted to lie above the Al atoms in the Al2 and Al3 layers, respectively. Models 9-11 consider a stacking fault such that the O1 layer is shifted to give an fcc stacking (*ABC*) to the topmost three O layers. In model 10, the Al1 layer sits in the three-fold hollow sites below which no atoms in the bulk structure occur. In model 11, the Al1 layer sits in the three-fold hollow sites above the O2 layer.
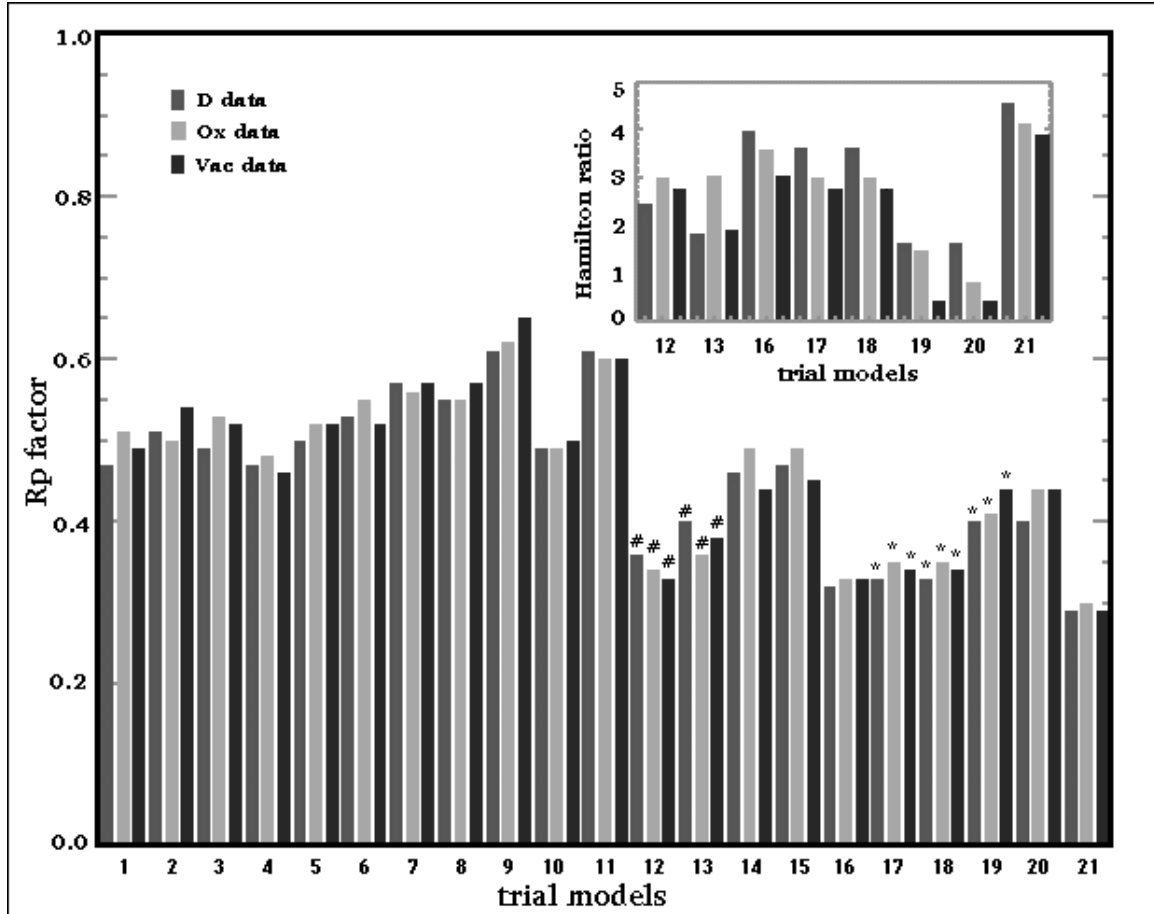
FIG. 4. Pendry R-factors (R_p) for the three α-Al$_2$O$_3$(0001) sample-preparation methods and the 21 models tested. The insert gives the Hamilton ratios (H_r) for the models having mixtures of two or more domain types (see Table 1). The models are numbered along the horizontal axis as: 1 – 5, ideal (0001) terminations; 6, water covered surface; 7 – 11, stacking faults; 12 – 15, single-species mirrored surfaces; 16 – 20, mixed-species terminations; and 21, split-position model. The stars in the figure note models whose optimized structures are close to those of the Al1+O1 model, despite the fact that the starting configurations were very different. The pound signs in

the figure note models that resulted in large, non-physical bond-lengths (e.g., a top layer expansion of 90%).
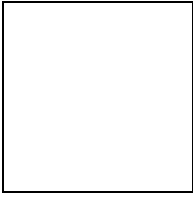
FIG. 5. Graphical representation of the atomic positions perpendicular to the surface in both terminations for the Al1-split and Al1+O1 models, compared to bulk values and to results from theory (A,[14] B,[11] and C[12]) and x-ray diffraction.[6] Each vertical line represents one termination and gives the optimized height of each atomic layer (labeled by individual layer-specific symbols) above the first fixed O layer (height = 0 Å). Pairs of connected lines correspond to pairs of terminations that were optimized together, showing resulting height differences.
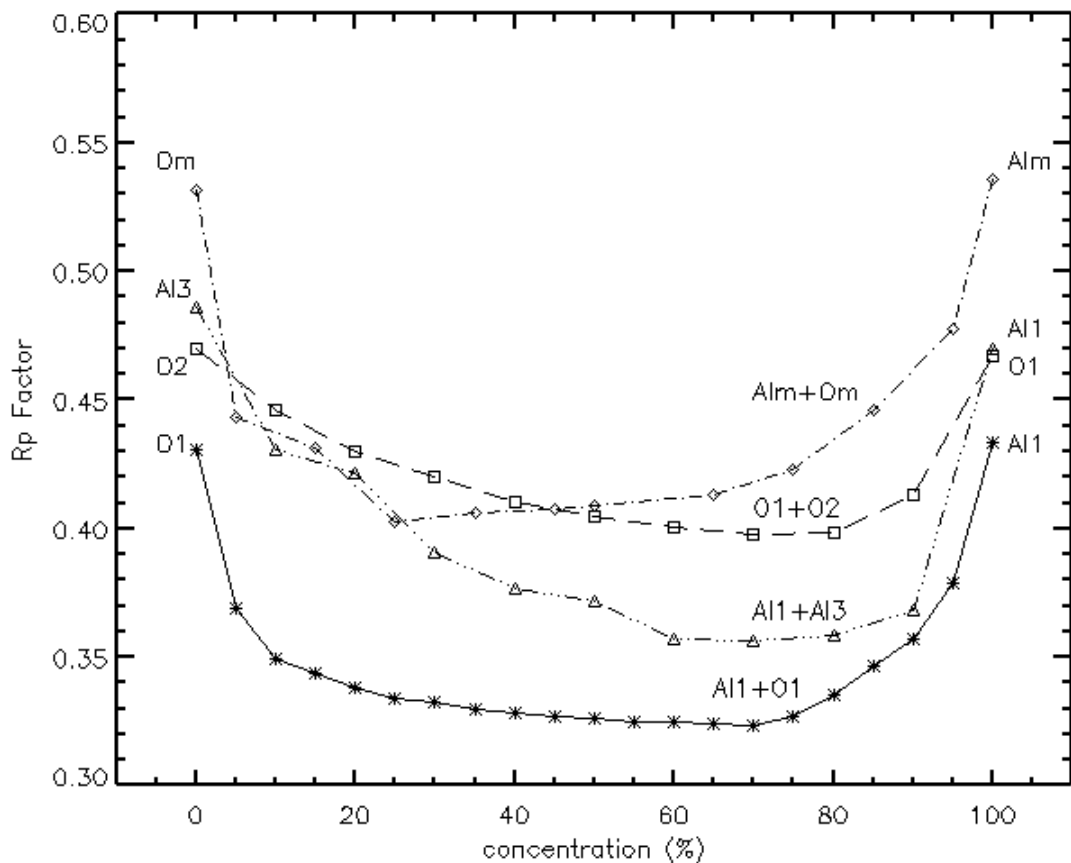
FIG. 6. The goodness of the model fits (Pendry R-factor, R_p) for representative surface models having a mixture of domains with different terminations. On the left-hand axis (0%) and the right-hand axis (100%), the models have a single domain of the labeled type. In between, the surface is a mixture of the two terminations. The extreme insensitivity to the domain concentration suggests that the mixed-domain classes of models are inappropriate. While the results shown are from the D experimental data set, the other surface preparations gave similar results.
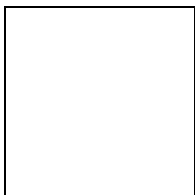
FIG. 7. Experimental (thin lines) and theoretical (thick lines) LEED I(V) curves for the split-position model for the Ox experimental data set. The (i,j) notation gives the index of the diffraction spots.
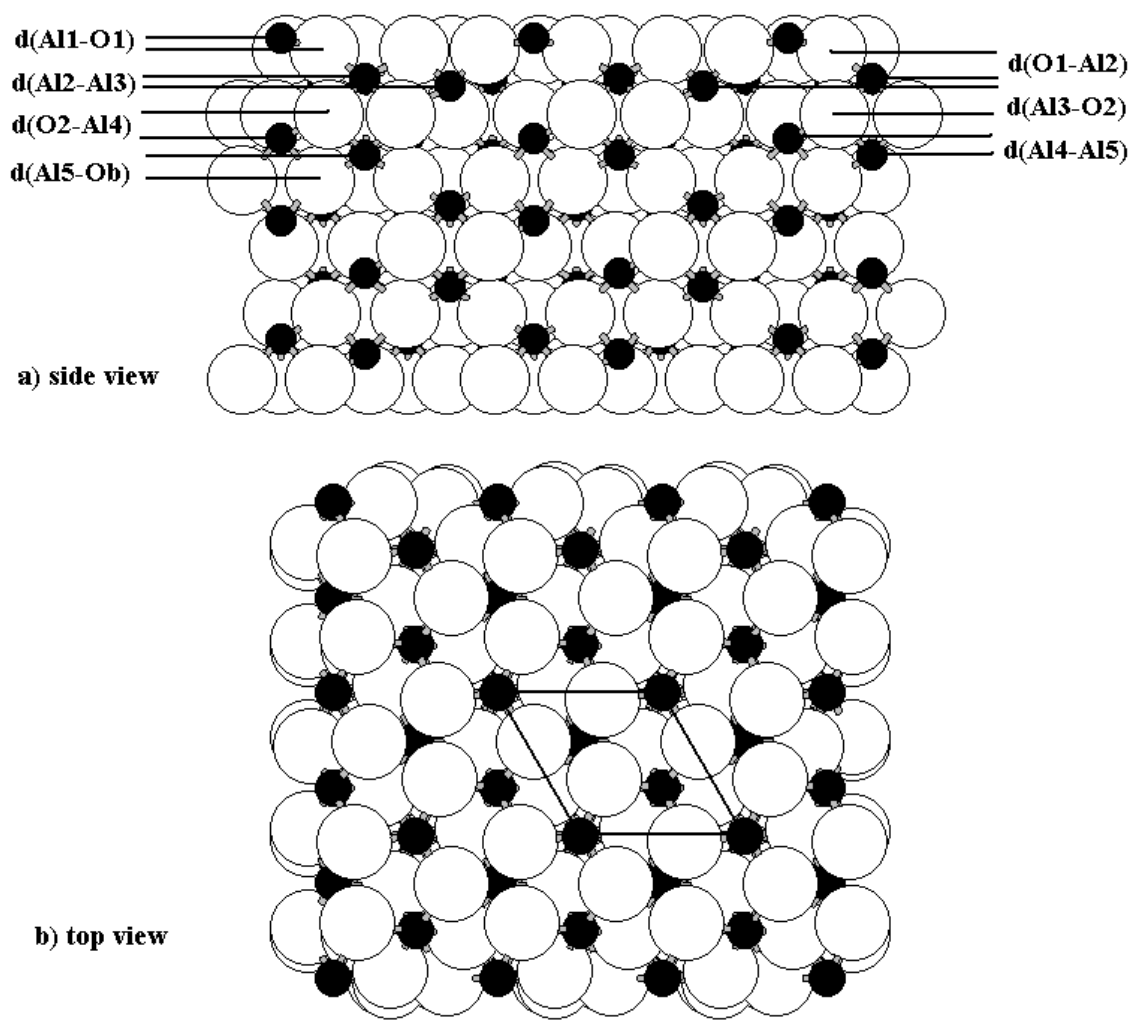
FIG. 8. Plan views of the best-fit structure (the split-position model, #21) of α-Al$_2$O$_3$(0001). Above: side view. Below: top view. The aluminum atoms are the small solid circles while the oxygen atoms are the large open circles.